*Int. J. Electrochem. Sci.*, 6 **(2011)** 3714 - 3728

**International Journal of ELECTROCHEMICAL SCIENCE**
www.electrochemsci.org

# Role of Iron Dopant and Carbon Additive in Improving the Ionic Transport and Electrochemical Properties of $LiFe_xMn_{1-x}PO_4$ (x=0.25 and 0.75) Solid Solutions

*D. Bhuvaneswari*[1], *Gangulibabu*[1], *Chil-Hoon Doh*[2,*], *N. Kalaiselvi*[1*]

[1] Central Electrochemical Research Institute, Karaikudi- 630 006, India
[2] Korea Electrotechnology Research Institute, Changwon 641-600, South Korea
[*]E-mail: chdoh@keri.re.kr and kalakanth2@yahoo.com

*Received:* 10 June 2011 / *Accepted:* 25 July 2011 / *Published:* 1 September 2011

Phase pure and nano crystalline solid solutions of select category $LiFe_{0.25}Mn_{0.75}PO_4$/C and $LiFe_{0.45}Mn_{0.55}PO_4$/C are synthesized using citric acid assisted sol-gel method with an addition of super P carbon as a conducting additive. Basically, the incorporation of Fe dopant is found to decrease the band gap of Mn-O-Mn linkage and the formation of mixed Fe-Mn based diffusion path of $LiFe_xMn_{1-x}PO_4$/C (x=0.25 and 0.45) improves lithium diffusion characteristics. Similarly, besides being a protective coating to impede the agglomeration of particles at high synthesis temperature (700 $^oC$), presence of amorphous carbon coating over native $LiFe_xMn_{1-x}Fe_xPO_4$/C particles offers an effective carbon wiring and enhanced electronic conductivity, desirable for facile lithium transport and better electrochemical properties. As a result, composite solid solutions of $LiFe_xMn_{1-x}PO_4$/C (x=0.25 and 0.45) type are found to exhibit enhanced conductivity and electrochemical properties. Particularly, $LiFe_{0.45}Mn_{0.55}PO_4$/C cathode exhibits significantly improved specific capacity of 132 mAh/g, due to the presence of higher concentration of Fe dopant. The synergistic effect of iron doping and super P carbon in improving the diffusion kinetics and electrochemical properties of the title compound are understood from the study.

**Keywords:** $LiMnPO_4$ cathode, ionic transport, solid solutions, super P carbon, lithium batteries

## 1. INTRODUCTION

Among the olivine $LiMPO_4$ (M=Mn, Fe, Co, and Ni) cathodes, classical $LiFePO_4$ has been studied extensively and thus leaves no great space for newer insights [1, 2]. On the other hand, $LiCoPO_4$ and $LiNiPO_4$ cathodes receive lesser attention due to the unprecedented volume expansion issues and the high voltage (≥ 5) red-ox range of $M^{3+}/M^{2+}$ couple [3]. In this regard, native $LiMnPO_4$, despite being an arguably interesting compound with respect to electrochemical properties is known

for its inherent safety, eco benign nature and the abundance of manganese on earth's crust [4]. As a result, investigation and fine tuning of physico-chemical properties that can be correlated to improve the electrochemical properties of modified $LiMnPO_4$ cathodes gains paramount importance, due to which surface and electronically modified $LiFe_xMn_{1-x}PO_4/C$ (x=0.25 & 0.45) cathodes have been chosen for the study.

Basically, reports on the promising perspectives of $LiMnPO_4$ cathode for use in rechargeable lithium batteries is very limited, due to the much slower lithium diffusion kinetics observed at C/200 rate [5]. It is well known that native $LiMnPO_4$ suffers from certain intrinsic frustrations like longer hopping distance of polarons of Mn-O-Mn linkage, larger unit cell volume (303.3 Å against 291.2 Å of $LiFePO_4$), larger spin exchange gap of 3 eV, internal friction of the bulk crystal of $LiMnPO_4/MnPO_4$ resulting from the large effective mass of polarons around $Mn^{3+}$ site coupled with large local lattice deformations that induces the blocking of one-dimensional lithium ion path of $LiMnPO_4$, poor electronic conductivity (~$10^{-10}$ S/cm) compared to $LiFePO_4$ (~$10^{-8}$ S/cm), $Mn^{2+}$ disorder [1, 5, 6-10] etc., due to which the electrochemical behaviour of the same poses numerous challenges to researchers.

With respect to the electrochemical properties of $LiMnPO_4$, despite the initial reports of Padhi *et al.* on the difficulty of extracting Li from $LiMnPO_4$, [1], specific capacity of 70 mAh/g at C/20 rate [5], 115 mAh/g at C/10 [11] and a controversially exceeding capacity of 140 mAh/g by Li *et al.* [12] are available in the literature. Recently Martha *et al.* have reported on the importance of nanosized material and conductive carbon coating to realize much improved specific capacity values [13], which is quite similar to the reported views of Goodenough *et al.* [1]. On the other hand, Yamada [6-10] and Molenda *et al.* [14, 15] have forecasted an alternative approach of preparing the solid solutions of $LiMnPO_4$, as a means of addressing the critical issues related to the electrochemical properties of $LiMnPO_4$. In this regard, Deyn Wang [16] and J.K. Kim *et al.* [17] have reported reasonably improved capacity values of 130 mAh/g ($LiMn_{0.9}Fe_{0.1}PO_4$ /C) and 155mAh/g ($LiMn_{0.4}Fe_{0.6}PO_4$/C) at C/10 rate. From a careful review of literature reports, it is understood that $LiFe_yMn_{1-y}PO_4$ solid solutions with a range of y=0.2~0.4 would exhibit acceptable electrochemical behavior [6-10].

Apart from the major focus on improving the specific capacity values, areas such as electrical and magnetic properties of $LiMnPO_4$, local structure of Li-Mn-Fe-$PO_4$ solid solutions and the effect of carbon composite upon diffusion mechanism and conductivity related issues remains less studied till date. Hence, the present study is aimed on the phase pure synthesis of nanocrystalline solid solutions of chosen category, viz. $LiFe_{0.25}Mn_{0.75}PO_4$ /C and $LiFe_{0.45}Mn_{0.55}PO_4$ /C and the investigation of ionic transport properties with a view to correlate the same with the observed electrochemical behavior. Herein, deployment of super P carbon with a conductivity of ~$10^2$ S/cm has been attempted in order to investigate the effort of carbon addition in increasing the ionic and electrical conductivity related lithium diffusion kinetics. Similarly, $LiFe_xMn_{1-x}PO_4/C$ compounds with x=0.25 and 0.45 have been chosen to understand the effect of concentration of iron dopant in improving the electrochemical behaviour of the native $LiMnPO_4$. Citric acid assisted sol-gel method has been used to synthesize the title compounds and the synergistic effect of carbon wiring and iron doping in facilitating facile lithium transport properties and improved electrochemical behaviour has been investigated.

## 2. EXPERIMENTAL SECTION

### *2.1. Synthesis*

$LiFe_xMn_{1-x}PO_4/C$ [x=0.25 (sample A) and 0.45 (sample B)] solid solutions were synthesized individually from stoichiometric ratios of starting materials, viz. lithium acetate, manganese acetate dihydrate, iron (II) oxalate and ammonium dihydrogen phosphate. Primarily, the reactants were mixed in hot water with stirring to get a homogeneous solution. To the solution, 1:1 molar ratio of citric acid and 10 wt. % super P carbon were added. The process of stirring and heating were continued to get a thick gel. The formed gels were dried individually at 110 °C and furnace-heated to 300 °C for about 8 h. and 700 °C for about 12 h. in Ar atmosphere with an intermittent grinding. The obtained fine powders of sample A and B were subjected to systematic physical and electrochemical characterization studies.

### *2.2. Physical and electrochemical characterizations*

Phase characterization was done by powder X-ray diffraction technique on a PANalytical X'pert PRO X-ray diffractometer using Ni-filtered Cu Kα radiation (λ = 1.5406 Å) in the 2θ range 10–$90^o$ at a scan rate of $0.04^\circ s^{-1}$. HRTEM was recorded using TECnai G2 F30 S-Twin TEM analyser. Total carbon content of the prepared materials was calculated from thermogravimetry analysis (TGA) performed with a thermo balance model STA 409 PC and the type of carbon coated over native compound is characterized by Renishaw Raman Spectrometer. Conductivity properties were studied using LCR meter (Hioki-3532) in the temperature range of 30 to 200 °C and in the frequency range of 42 to 1MHz. Cyclic voltammetry studies were carried out using an Auto lab electrochemical workstation and the charge-discharge studies were carried out using MACCOR charge-discharge cycle life tester.

### *2.3. Electrode preparation and cell assembly*

Details pertaining to electrode fabrication and 2032 coin cell assembly are reported elsewhere [18]. Electrochemical characterizations were carried out on freshly fabricated 2032 coin cells consisting of lithium anode, synthesized cathode and a non-aqueous electrolyte containing 1M $LiPF_6$ dissolved in 1:1 v/v EC:PC with a celgard separator.

## 3. RESULTS AND DISCUSSION

### *3.1. Structural analysis by PXRD*

The crystal phase of synthesized $LiFe_xMn_{1-x}PO_4/C$ [x=0.25(sample A) and 0.45 (sample B)] is identified to be $LiMnPO_4$ (Fig. 1) with an ordered olivine structure and an orthorhombic Pnmb space group corresponding to ICCD pattern No: 01-077-0178.

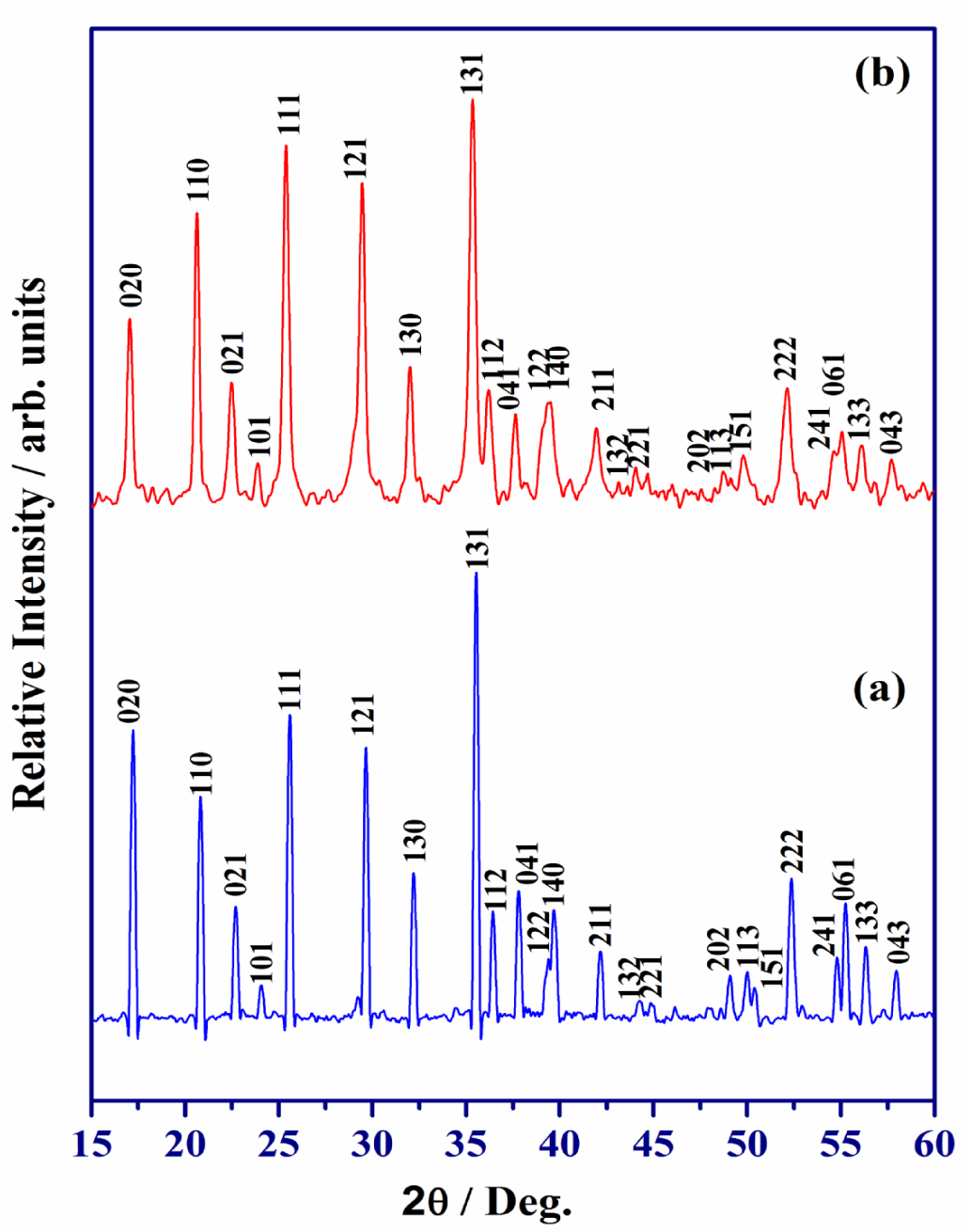


**Figure 1.** XRD pattern observed for a) $LiFe_{0.25}Mn_{0.75}PO_4/C$ and b) $LiFe_{0.45}Mn_{0.55}PO_4/C$

Absence of impurity peaks confirms the phase pure formation of $LiFe_{0.25}Mn_{0.75}PO_4/C$ and $LiFe_{0.45}Mn_{0.55}PO_4/C$ synthesized by citric acid assisted sol-gel method. Substitution of smaller $Fe^{2+}$ ions [92 pm] in $Mn^{2+}$ site [97 pm] decreases the lattice parameter value, as understood from the lower value observed for $LiFe_{0.45}Mn_{0.55}PO_4/C$ (a=10.336, b=6.025 and c= 4.693) compared to that of $LiFe_{0.25}Mn_{0.75}PO_4/C$ (a=10.447, b=6.1016 and c= 4.750). The appearance of well broadened bragg peaks evidences the nanocrystalline nature of synthesized compounds and the calculated grain boundary is around 28 nm. Further, the stoke's strain value is calculated to be $2.4x10^{-3}$ for $LiFe_{0.25}Mn_{0.75}PO_4/C$ and $1.8x10^{-3}$ for $LiFe_{0.45}Mn_{0.55}PO_4/C$ compounds.

*3.2. Carbon coating by HRTEM and carbon content by TGA*

Presence of continuous and uniform coating of carbon over the grain boundary of $LiFe_{0.25}Mn_{0.75}PO_4$ /C and $LiFe_{0.45}Mn_{0.55}PO_4$/C nanocomposites is obvious from the recorded HRTEM images (Fig. 2a and b).

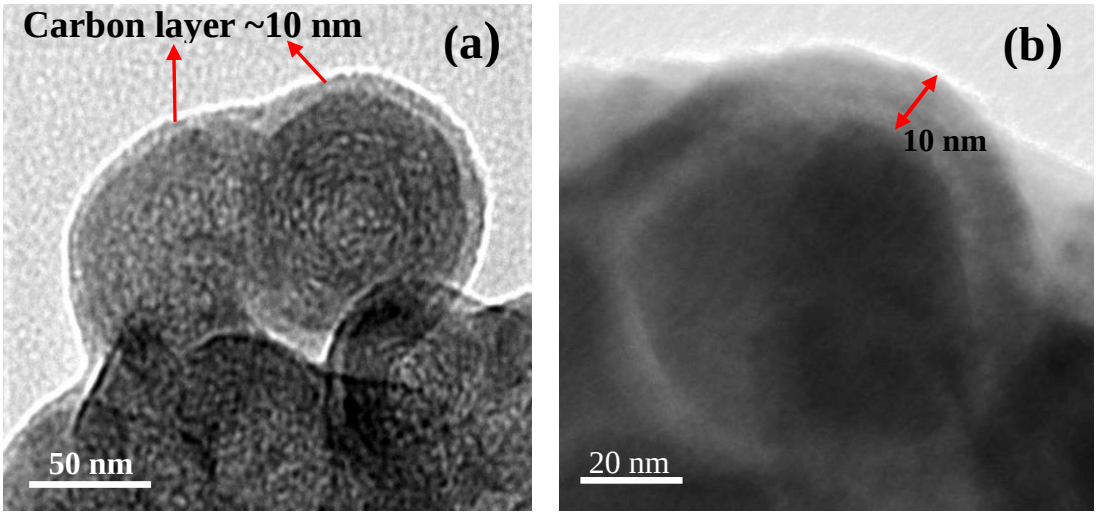


**Figure 2.** HRTEM images of sol-gel synthesized a) $LiFe_{0.25}Mn_{0.75}PO_4$/C and b) $LiFe_{0.45}Mn_{0.55}PO_4$/C

The synergistic effect of added 10 wt.% Super P carbon and the residual carbon resulting from citric acid assisted sol-gel method is found to be advantageous in controlling the growth of particles of samples A and B and to provide a protective coating. Presence of nanocrystalline $LiFe_xMn_{1-x}PO_4$/C (x=0.25 and 0.45) solid solutions with a particle size of ~50 nm is understood from Figs. 2a and b. More interestingly, presence of carbon wiring that connects the individual grains is expected to increase the electronic conductivity and the related lithium transport kinetics of samples A and B. Further, total carbon content of $LiFe_{0.25}Mn_{0.75}PO_4$/C and $LiFe_{0.45}Mn_{0.55}PO_4$/C compounds is calculated to be ~20 wt. % from TG/DTA results, an indication that residual carbon resulting from the decomposition of citric acid increases the total carbon content of the composites.

*3.3. Surface property by Raman Spectroscopy*

Since the electrochemical performance of composite electrode depends upon the type of carbon involved, samples A and B were subjected to Raman spectroscopy. The recorded spectra **(**Fig. 3a and b) show two characteristic broad bands around 1585 (G-band) and 1340 $cm^{-1}$ (D band), corresponding to the presence of ordered graphitic carbon and the amorphous carbon [19, 20] respectively. The $I_D/I_G$ intensity ratio is found to be negligible (0.02), thus representing the degree of decreasing $sp^3$ /$sp^2$ carbon ratio. In otherwords, the observed carbon coating is due to the presence of $sp^2$ hybridized carbon, which is reported to be favourable to enhance the electrochemical behavior of lithium intercalating cathode materials [21, 22]

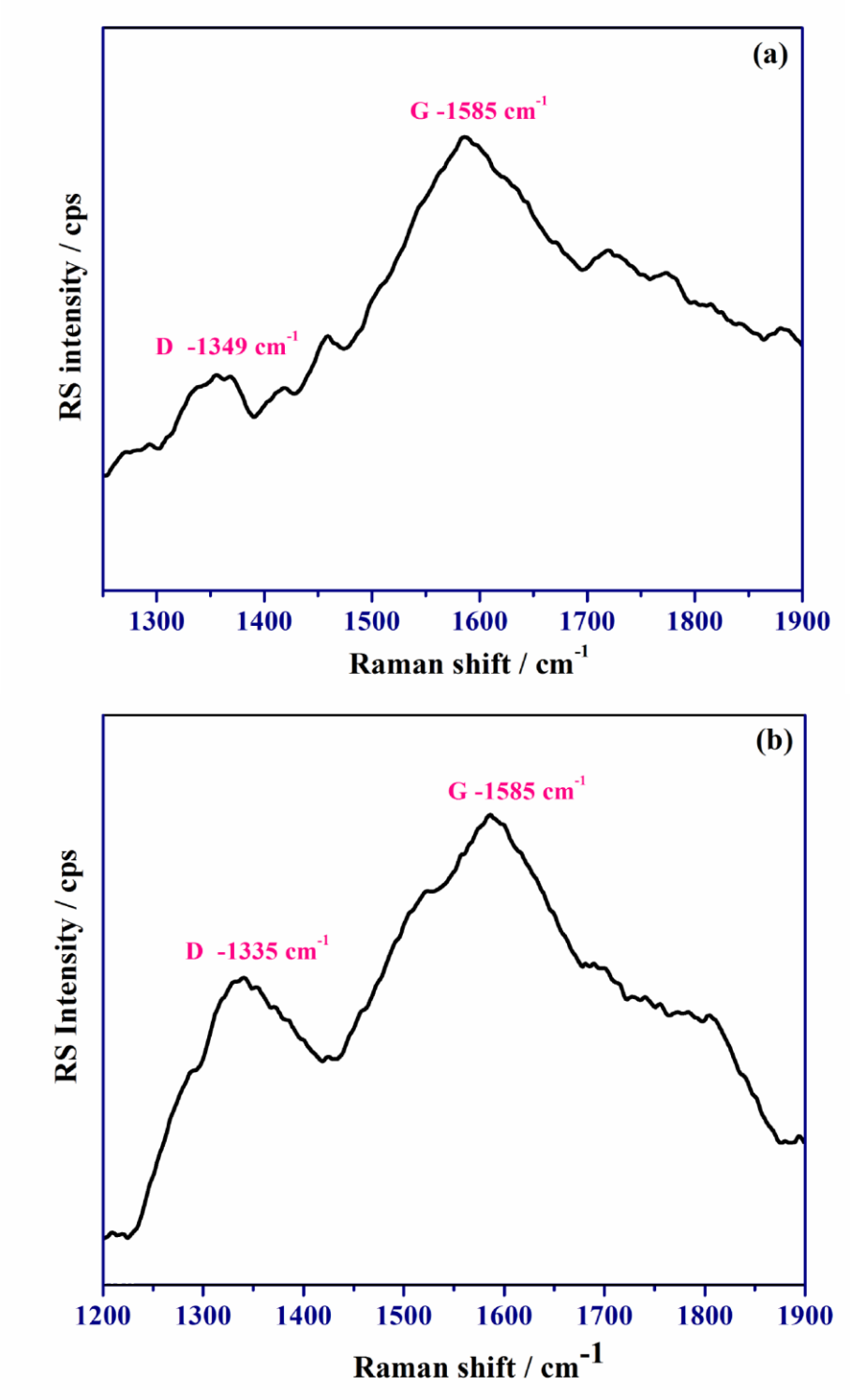


**Figure 3**. Raman spectra of a) $LiFe_{0.25}Mn_{0.75}PO_4$/C and b) $LiFe_{0.45}Mn_{0.55}PO_4$/C

*3.4. Ionic conductivity studies*

$LiFe_{0.25}Mn_{0.75}PO_4$ /C and $LiFe_{0.45}Mn_{0.55}PO_4$/C nanocomposites were further subjected to ionic transport characterization studies with a view to understand the role of iron dopant ,effect of super P carbon and the citric acid assisted sol-gel method in improving the transport kinetics of $Li^+$ diffusion

via. reduced band gap energy and enhanced electronic conductivity. As expected, Arrhenius plot (Fig. 4) shows significantly improved ionic conductivity values of 8.9 $x10^{-6}$ and 1.56 $x10^{-6}$ for samples A and B respectively, which is four times higher than the reported value [14, 15].

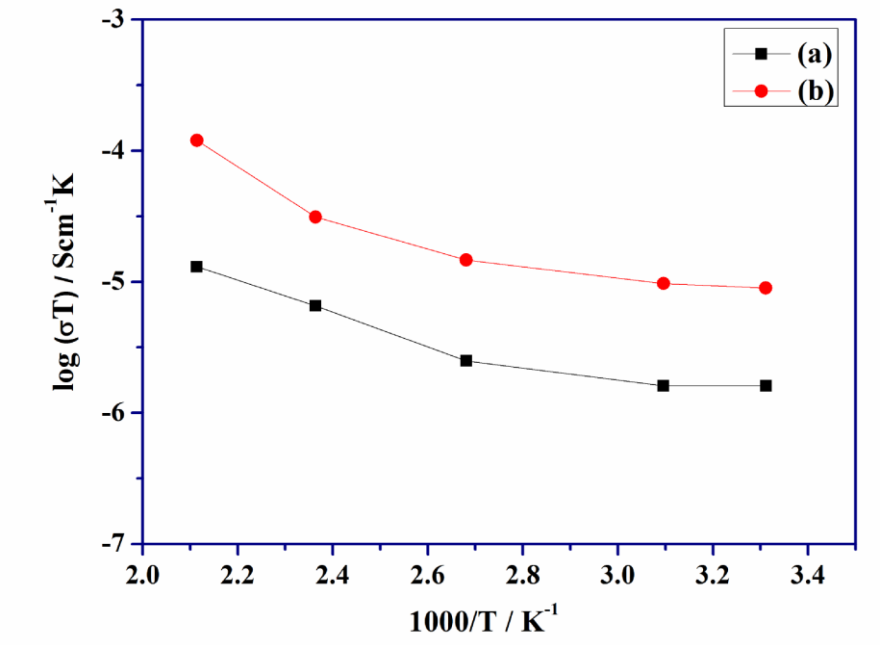


**Figure 4.** Arrhenius plot of a) $LiFe_{0.25}Mn_{0.75}PO_4/C$ and b) $LiFe_{0.45}Mn_{0.55}PO_4/C$

**Table 1.** Conductivity parameters of $LiFe_{0.25}Mn_{0.75}PO_4/C$ (sample A) $LiFe_{0.45}Mn_{0.55}PO_4/C$ (sample B) measured at various temperatures

| Temp. °C | Sample A | | | | Sample B | | | |
|---|---|---|---|---|---|---|---|---|
| | Bulk resistance (Rb) | σdc ($Scm^{-1}$) | Hoping frequency | K | Bulk resistance (Rb) | σdc ($Scm^{-1}$) | Hoping frequency | K |
| 30 | $2.18X10^4$ | $1.56\ X10^{-6}$ | $1.78\ X10^5$ | $1.52\ X10^{-8}$ | $1.24X10^5$ | $8.90X10^{-6}$ | $3.11\ X10^4$ | $8.25\ X10^{-8}$ |
| 50 | $2.04X10^4$ | $1.57\ X10^{-6}$ | $1.91\ X10^5$ | $1.62\ X10^{-8}$ | $7.93X10^4$ | $9.55\ X10^{-6}$ | $3.14\ X10^4$ | $9.72\ X10^{-8}$ |
| 100 | $1.34X10^4$ | $2.44\ X10^{-6}$ | $2.86\ X10^5$ | $1.87\ X10^{-8}$ | $2.97X10^4$ | $1.43\ X10^{-5}$ | $4.88\ X10^4$ | $1.17\ X10^{-7}$ |
| 150 | $6.16X10^3$ | $6.51\ X10^{-6}$ | $6.18\ X10^5$ | $2.12\ X10^{-8}$ | $1.14X10^4$ | $3.09\ X10^{-5}$ | $1.30\ X10^5$ | $3.32\ X10^{-7}$ |
| 200 | $1.48X10^3$ | 1.61 X10-5 | $2.38\ X10^6$ | $2.37\ X10^{-8}$ | $3.36X10^3$ | $1.18\ X10^{-4}$ | $3.23\ X10^5$ | $4.72\ X10^{-7}$ |
| 250 | $8.03X10^2$ | $4.91\ X10^{-5}$ | $4.58\ X10^6$ | $2.62\ X10^{-8}$ | $5.13X10^2$ | $2.28\ X10^{-4}$ | $9.82\ X10^5$ | $4.98\ X10^{-7}$ |
| 300 | $4.02X10^2$ | $1.46\ X10^{-4}$ | $9.48\ X10^6$ | $2.87\ X10^{-8}$ | $4.33X10^2$ | $4.78\ X10^{-4}$ | $2.93\ X10^6$ | $6.79\ X10^{-7}$ |

The linear variation of conductivity values as a function of increasing temperature has been studied and the same is tabulated (Table. 1). From the table, it is understood that with the increasing temperature, the semiconducting solid solutions (A and B) acquire some activation energy, sufficient to cross the potential barrier between the conduction and valence band [23-26] and thereby exhibiting increased conductivity values. Herein, the longer hopping distance of polarans pertinent to Mn-O-Mn

linkage in $LiMnPO_4$ is shortened slightly both by the formation of Li-Fe-Mn-O and by reducing the size of the particles with a conductive carbon coating. Particularly, the effect of Fe doping is found to decrease the larger spin-exchange gap of native $LiMnPO_4$ considerably, as the same is understood from the much reduced hopping frequency of $LiFe_{0.45}Mn_{0.55}PO_4/C$ compound containing higher concentration of Fe dopant.

### *3.5. Impedance measurement*

Impedance analysis over a wide range of frequency and as a function of increasing temperature has been carried out to understand the extent of charge transport processes taking place particularly in between the grains of the composite cathode.

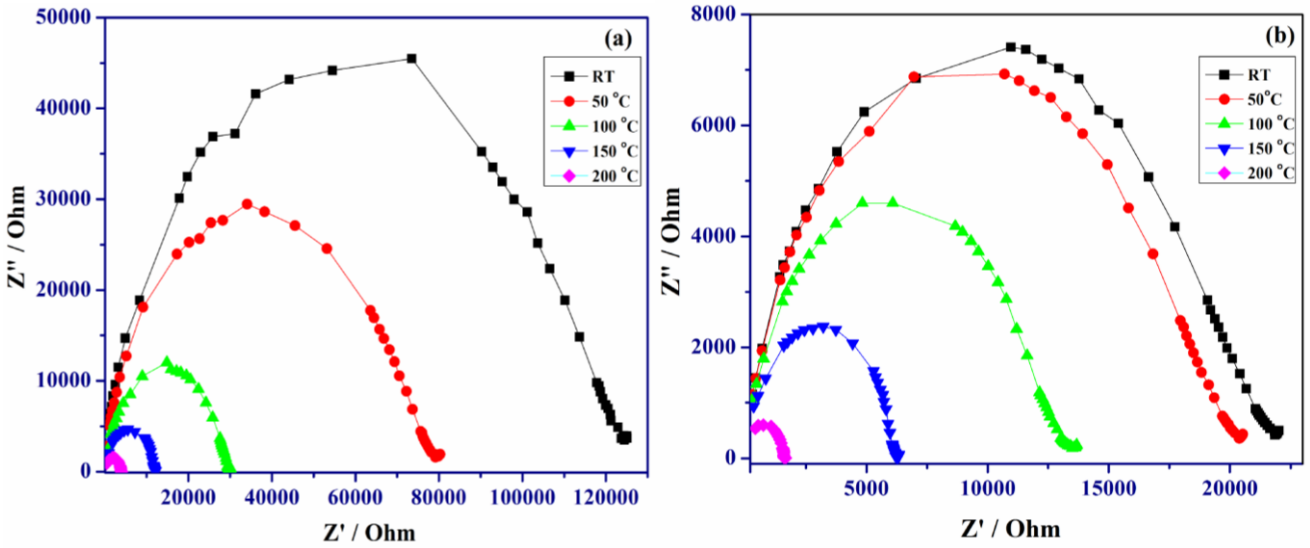


**Figure 5.** Variation of relaxation time as a function of temperature exhibited by a) $LiFe_{0.25}Mn_{0.75}PO_4/C$ and b) $LiFe_{0.45}Mn_{0.55}PO_4/C$

Fig. 5 shows the variation of relaxation time in the form of a semi circle that decreases with an increase in temperature. All the cole-cole plots contain a single semicircle with its centre lies below the real axis at high frequencies [23-26], which is an indication of resistance due to particle-particle interaction. The bulk resistance ($R_b$) can be calculated from the lower frequency interaction at the real axis and the associated capacitance can be calculated from the maximum of the semicircle using the relation $\omega R_b C_b = 1$ [23-26]. The calculated values are furnished in Table.1. At room temperature, $LiFe_{0.45}Mn_{0.55}PO_4/C$ exhibits lower bulk resistivity than $LiFe_{0.25}Mn_{0.75}PO_4/C$, which is understood from the modified conduction path in the crystal lattice of the same facilitated by the higher concentration of Fe dopant. The difference between the intercepts of the high and low-frequency region that corresponds to the grain boundary conductivity is found to be less for samples A & B, thus demonstrating the presence of good inter-particle contact developed by the conducting carbon network resulting from the composite cathodes.

*3.6. Frequency dependent conductivity*

The effect of incorporation of Fe as a dopant to minimise the spin exchange gap and the unit cell volume of native $LiMnPO_4$ has been investigated as a function of concentration of Fe dopant and as a measure of conductivity. More precisely, the combined effect of dopant and the nanocrystalline nature of composite solid solution with carbon coating has been evaluated by ionic conductivity measurements (Fig. 6).

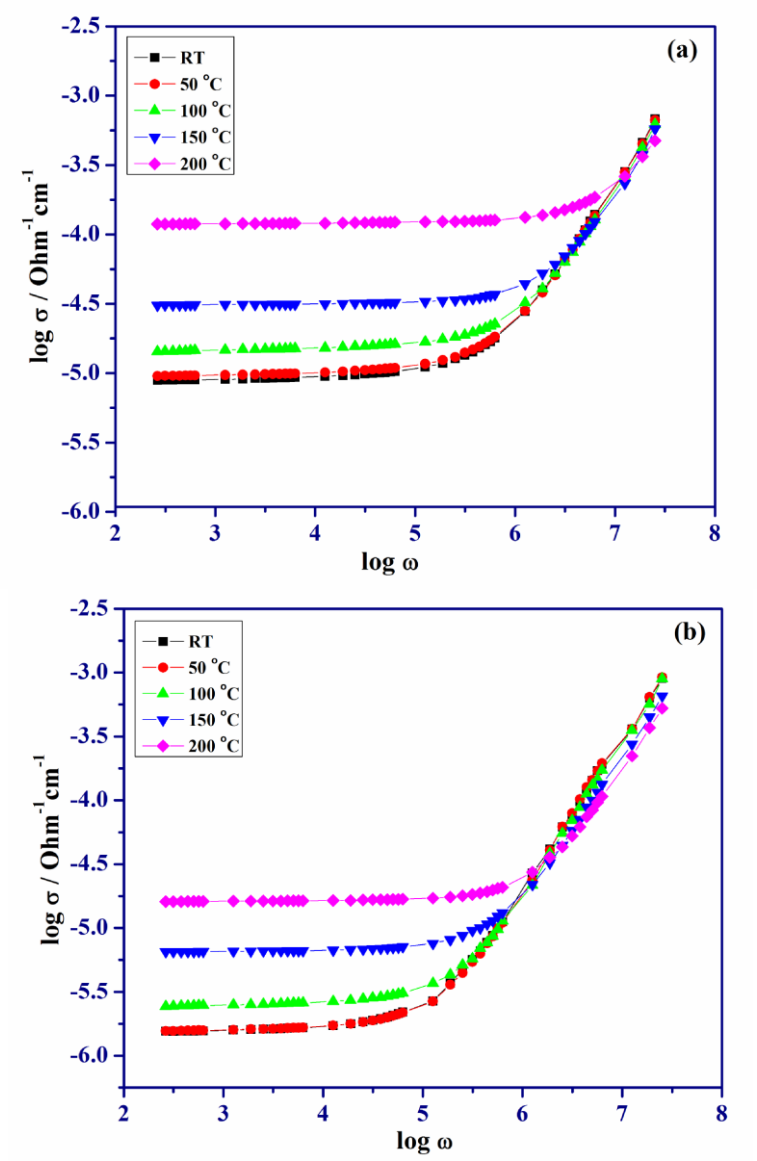


**Figure 6.** Conductance plot of a) $LiFe_{0.25}Mn_{0.75}PO_4/C$ and b) $LiFe_{0.45}Mn_{0.55}PO_4/C$

The larger effective mass of the polarons around $Mn^{3+}$ sites coupled with larger local lattice deformations related to native $LiMnPO_4$ that results in the blocking of one dimensional lithium diffusion path and slows down the diffusion kinetics is found to get addressed, especially with the combination of Fe dopant, as evidenced by the increased values of conductivity (Table. 1). As a result,

the activation energy required for $LiFe_{0.45}Mn_{0.55}PO_4/C$ (0.317 eV) is quite lesser than $LiFe_{0.25}Mn_{0.7}PO_4/C$ (0.456 eV), supported duly by the enhanced conductance value and hopping rate of the former than later.

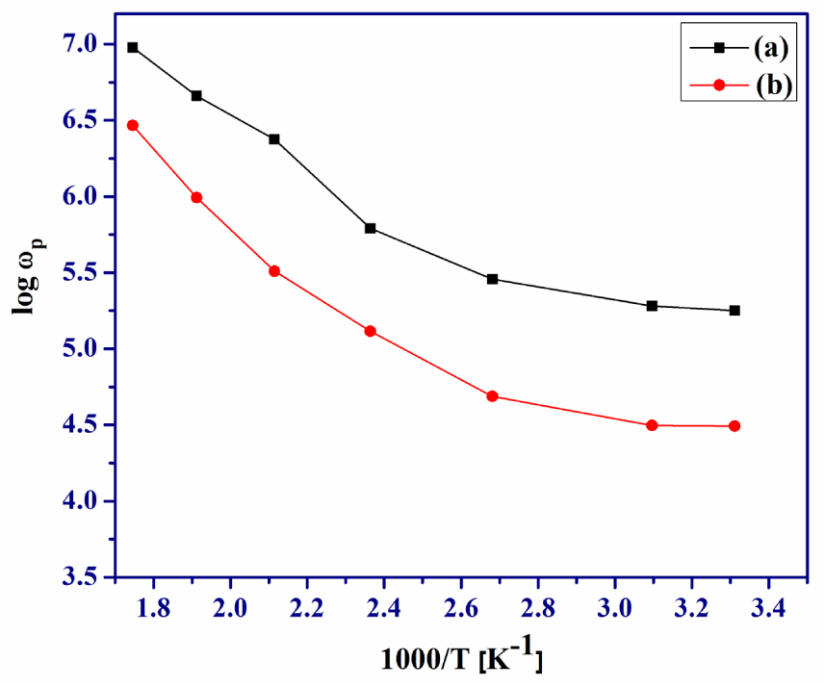


**Figure 7**. Variation of Hoping rate with respect to temperature a) $LiFe_{0.25}Mn_{0.75}PO_4/C$ and b) $LiFe_{0.45}Mn_{0.55}PO_4/C$

Fig. 7 evidences the increasing hoping rates observed with respect to samples A and B that varies linearly with the increasing temperature. Since ion hoping rate is thermally activated, it can be calculated by

$$\omega_p = \omega_e \exp (H_m/kT)$$

where $\omega_e$ is the effective frequency and $H_m$ is the activation enthalpy for hopping. $H_m$ is determined from the slope of the temperature dependent ion hopping rate plot, which is closer to the activation energy value. Among the two samples, $LiFe_{0.45}Mn_{0.55}PO_4/C$ exhibits enhanced hopping rate due to the significantly reduced activation energy of the same, facilitated by higher concentration of Fe dopant.

### *3.8. Electrochemical studies*

Based on the encouraging results obtained from ionic conductivity studies of samples A and B, CV study was performed with the 2032 coin cells fabricated with the corresponding electrodes (0.1 mV/sec). Unlike native $LiMnPO_4$, the voltammograms of $LiFe_{0.25}Mn_{0.75}PO_4/C$ and

$LiFe_{0.45}Mn_{0.55}PO_4/C$ (Fig. 8) represent the characteristic mixed Fe-Mn phosphate behaviour, typical of $LiFePO_4$ (a couple of peaks centered at 3.5/3.4 V *vs.* Li) and of $LiMnPO_4$ (a couple of peaks centered around 4.1/3.9 V *vs.* Li).

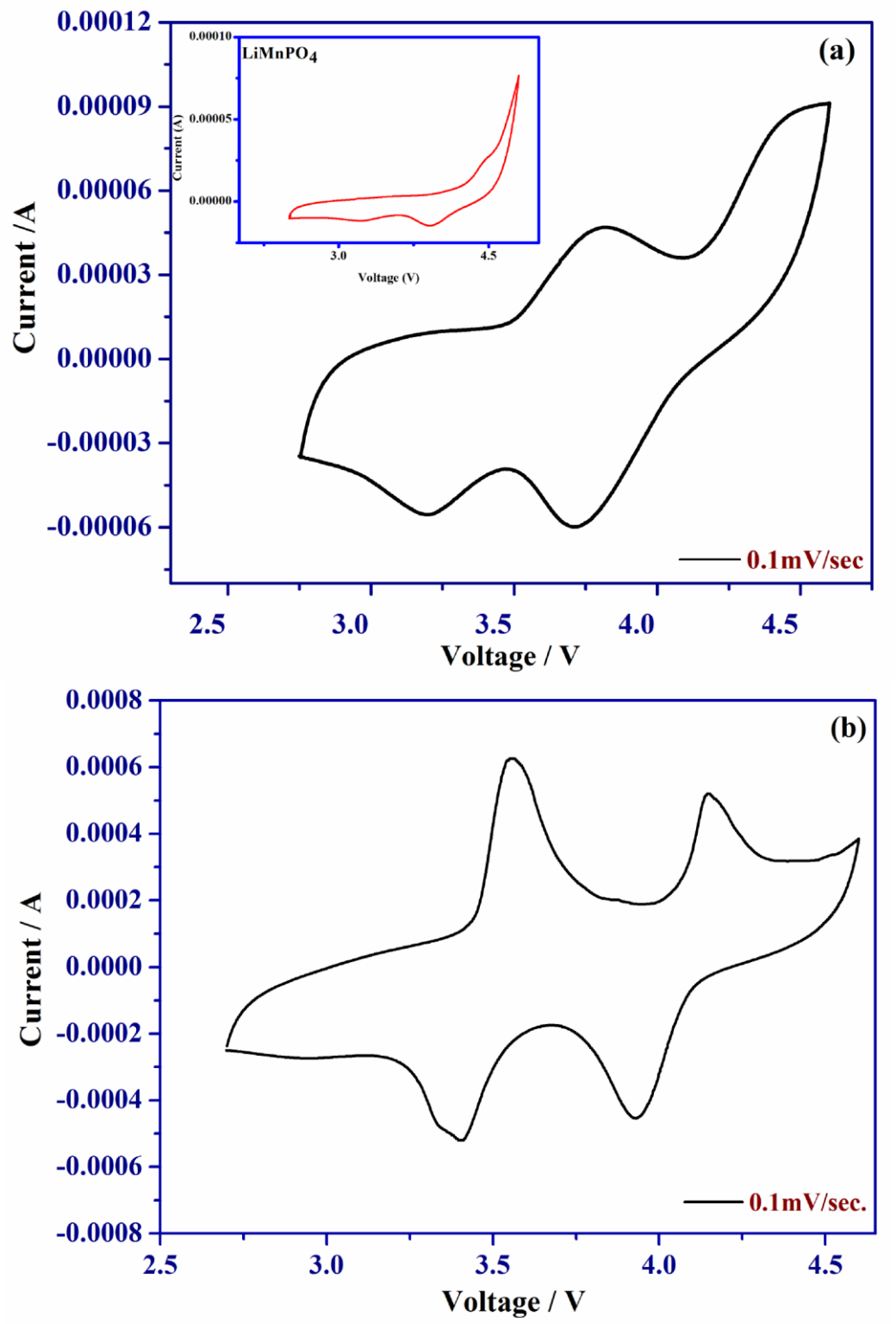


**Figure 8.** Cyclic Voltammogram of a) $LiFe_{0.25}Mn_{0.75}PO_4/C$ and b) $LiFe_{0.45}Mn_{0.55}PO_4/C$ cathode; Inset of (a**):** CV behavior of native $LiMnPO_4$

During the cathodic sweep, $Mn^{3+}$ is reduced to $Mn^{2+}$ around 4.1 V and $Fe^{3+}$ to $Fe^{2+}$ around 3.5 V [1], thus evidencing the formation of solid solution without exceeding the limit. Further, the increased peak current values of $LiFe_{0.45}Mn_{0.55}PO_4/C$ is in favour of improved electrochemical behavior and in particular the possibility of exhibiting higher specific capacity value compared to that of $LiFe_{0.25}Mn_{0.75}PO_4/C$, as indicated by the conductivity measurement studies.

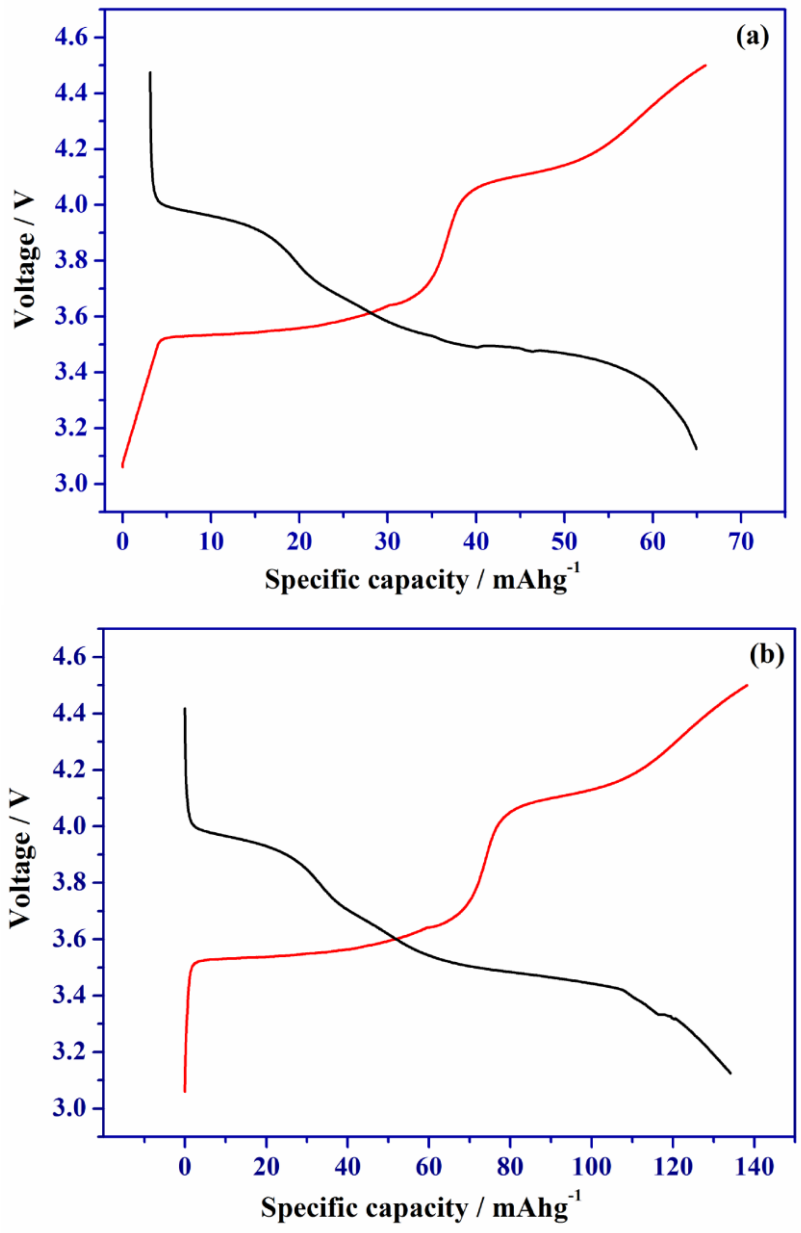


**Figure 9.** Typical Charge-discharge profile for the voltage range of 3.0-4.5V a) $LiFe_{0.25}Mn_{0.75}PO_4/C$ b) $LiFe_{0.45}Mn_{0.55}PO_4/C$ cathode

Fig. 9 represents the charge-discharge behaviour of $LiFe_{0.25}Mn_{0.75}PO_4/C$ and $LiFe_{0.45}Mn_{0.55}PO_4/C$ cathodes, wherein plateau region corresponding to $Fe^{3+}/Fe^{2+}$ (3.5V) and $Mn^{3+}/Mn^{2+}$(4.1V) redox reactions are seen clearly. The negligible difference observed between the

charge and discharge curves of composite cathodes (A and B) is in favour of enhanced coulombic efficiency, desirable for lithium intercalating cathodes. Here again, an enhanced discharge capacity of 132mAh/g has been exhibited by $LiFe_{0.45}Mn_{0.55}PO_4$/C, from which advantageous effect of higher concentration of Fe dopant is clearly understood. However, the effect of conducting carbon coating is found to improve the specific capacity of $LiFe_{0.25}Mn_{0.75}PO_4$ /C cathode nominally from 30mAh/g (native $LiMnPO_4$) to 65mAh/g, which is interesting.

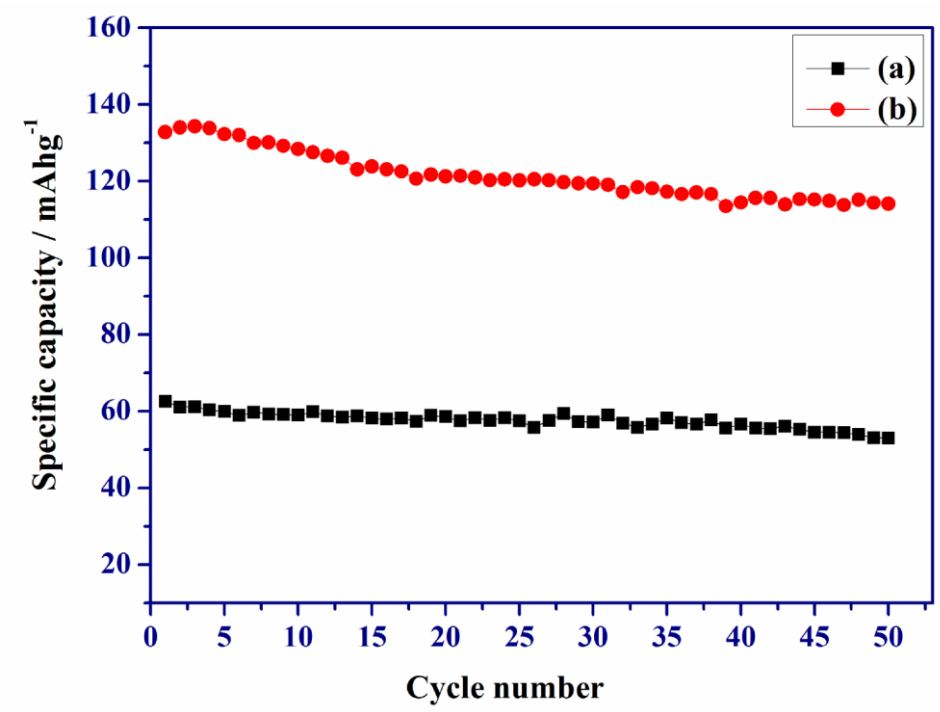


**Figure 10.** Specific discharge capacity *vs.* Cycle number of a) $LiFe_{0.25}Mn_{0.75}PO_4$/C b)$LiFe_{0.45}Mn_{0.55}PO_4$/C cathode

Variation of specific capacity of $LiFe_{0.25}Mn_{0.75}PO_4$/C and $LiFe_{0.45}Mn_{0.55}PO_4$/C cathodes with cycle number is depicted in Fig. 10. From the figure, it is evident that an appreciable specific capacity of 132mAh/g with a capacity fade of 11% is obtained for $LiFe_{0.45}Mn_{0.55}PO_4$/C cathode for 50cycles. On the other hand, an inferior specific capacity of 62mAh/g with less than 15% capacity fade has been exhibited by $LiFe_{0.25}Mn_{0.75}PO_4$/C cathode. The comparatively higher specific capacity of 132mAh/g exhibited by $LiFe_{0.45}Mn_{0.55}PO_4$/C cathode is comparable with the reports of J-K Kim *et al.* [17] for similar solid solutions and is superior than the results of D. Wang *et al.* [16] reported for solid solutions containing different dopants in the place of Mn in $LiMnPO_4$. Unlike native $LiMnPO_4$, the reduced capacity fade behavior observed with the solid solutions (A and B) of the present study is attributed to the effective carbon wiring provided by the addition of highly conducting super P carbon and the residual carbon that offers protective coating against undesirable side reactions with the electrolyte and promotes facile lithium diffusion kinetics. Particularly, the higher concentration of Fe plays an additional role of increasing the activation energy via. reduced hopping distance of M-O-M

linkage, as discussed earlier. Hence, it is understood from the study that $LiFe_{0.45}Mn_{0.55}PO_4$/C cathode experiences the overall advantages of carbon wiring and Fe doping induced improved lithium transport kinetics.

## 4. CONCLUSION

Tailor-made solid solutions of $LiFe_{0.25}Mn_{0.75}PO_4$ /C and $LiFe_{0.45}Mn_{0.55}PO_4$ /C are synthesized by citric acid assisted sol-gel method using super P carbon as conducting additive. Presence of nanocrystalline particles and the formation of continuous and uniform coating of carbon over $LiFe_xMn_{1-x}PO_4$/C (x=0.25 and 0.45) solid solutions are evident from the observed HRTEM images. The total carbon content is found to be ~ 20wt. % and the presence of desirable $sp^2$ hybridized carbon has been confirmed. The detailed investigation of ionic conductivity, impedance measurement and frequency dependent conductivity studies are in favor of the fact that the concentration of Fe dopant and the conducting carbon improve the transport kinetics of lithium diffusion in a significant manner. The distinct appearance of characteristic CV peaks evidences the presence mixed Fe-Mn phosphate behaviour and an enhanced discharge capacity of 132 mAh/g has been exhibited by $LiFe_{0.45}Mn_{0.55}PO_4$/C cathode. The reduced capacity fade behavior of title cathodes results from an effective and protective carbon coating, aided by the addition of super P carbon. Among the chosen candidates, $LiFe_{0.45}Mn_{0.55}PO_4$/C cathode enjoys the synergistic advantages of carbon wiring, Fe doping and improved lithium transport kinetics, thus qualifying itself as a better candidate of choice for futuristic applications.

ACKNOWLEDGEMENT
The authors are thankful to CSIR, India for financial support to carry out this work through the Inter Agency Project [IAP-04] of CECRI.

## References

1. A.K. Padhi, K.S. Nanjundaswamy, J.B. Goodenough, *J. Electrochem. Soc*.144 (1997) 1188.
2. K. Amine, H. Yasuda, and M. Yamachi, *Electrochem. Solid- State Lett.* 3 (1997) 178.
3. P. Deniard, A.M. Dulac, X. Rocquefelte, V. Grigorova, O. Lebacq, A. Pasturel, S. Jobic, *J. Phys. Chem. Solids*. 65 (2004) 229.
4. J. M. Tarascon and M. Armand, *Nature*. 414 (2001) 359.
5. C. Delacourt, P. Poizot, M. Morcrette, J.-M. Tarascon, and C. Masquelier, *Chem. Mater.* 16 (2004) 93.
6. A.Yamada, Y. Kudo, K. Liu, *J. Electrochem. Soc.* 148 (2001) A747.
7. A.Yamada and S. Chung, *J. Electrochem. Soc*. 148 (2001) A960.
8. A.Yamada, Y. Kudo, and K. Liu, *J. Electrochem. Soc.* 148 (2001) A1153.
9. Masao Yonemura, Atsuo Yamada, Yuki Takei, Noriyuki Sonoyama, and Ryoji Kanno, *J.Electrochem. Soc.,* 151 (9) A1352-A1356 (2004)

10. A.D. Morgan, A .Van der Ven, G. Ceder, *Electrochem. Solid- State Lett*. 7 (2004), A30. 11. Deyu Wang, Hilmi Buqa, Michael Crouzet, Gianluca Deghenghi, Thierry Drezen, Ivan Exnar, Nam-Hee Kwon, James H. Miners, Laetitia Poletto, Michael GrätzeL, *J. Power Sources.* 189 (2009) 624.
11. Guohua Li, Hideto Azuma, and Masayuki Tohda, *J. Electrochem. Soc.* 149 (2002) A743.
12. S. K. Martha,a B. Markovsky, J. Grinblat, Y. Gofer,O. Haik, E. Zinigrad, D. Aurbach, T. Drezen, D. Wang, G. Deghenghi, and I. Exnar, *J. Electrochem. Soc.* 156 (2009) A541.
13. J. Molenda, W. Ojczyk, J. Marzec, *J. Power Sources*. 174 (2007) 689.
14. J. Molenda, W. Ojczyk, K. Swierczek, W. Zajac. F. Krok, J. Dygas, Ru-Shi Liu, *Solid State Ionics*. 177 (2006) 2617.
15. Deyu Wang, Chuying Ouyang, Thierry Drézen, Ivan Exnar, Andreas Kay, Nam-Hee Kwon, Pascal Gouerec, James H. Miners, Mingkui Wang, and Michael Grätzela, *J.Electrochem. Soc.*157 (2010) A225.
16. Jae-Kwang Kima, Ghanshyam S. Chauhana, Jou-Hyeon Ahna, Hyo-Jun Ahnb, *J. Power Sources*.189 (2009) 391.
17. Gangulibabu, N. Kalaiselvi, D. Bhuvaneswari, C. H. Doh, *Int. J. Electrochem. Sci.* 5 (2010) 1597.
18. M. Doeff, Y. Hu, F. McLarnon, R. Kostecki, *Electrochem. Solid State Lett.* 6 (2003) A207.
19. Y. Hu, M. Doeff, R. Kostecki, R. Finones, *J. Electrochem. Soc.* 151 (2004) A1279.
20. J.W. Fergus, *J. Power Sources*. 195 (2010) 939.
21. A.K. Jonsher, *Nature.* 267 (1977) 673.
22. E.F. Hairetdinov, N.F. Uvarov, *Phys. Rev B. Condens. Matter*. 50 (1994) 259.
23. W.D. Kingery, *Introduction to Ceramics, 2nd ed., John Wiley, New York* (1976) 938.
24. A.Orilukas, A. Dindune, Z. Kanepe, J. Ronis, E. Kazakevicius, A.Kezionis, *Solid State Ionics* 157 (2003) 177.